REGULAR ARTICLE

blood advances

Sipa1 deficiency–induced bone marrow niche alterations lead to the initiation of myeloproliferative neoplasm

Pingnan Xiao,[1] Monika Dolinska,[1] Lakshmi Sandhow,[1] Makoto Kondo,[1] Anne-Sofie Johansson,[1] Thibault Bouderlique,[1] Ying Zhao,[2,3] Xidan Li,[4] Marios Dimitriou,[1] George Z. Rassidakis,[5] Eva Hellström-Lindberg,[1] Nagahiro Minato,[6] Julian Walfridsson,[1] David T. Scadden,[7-9] Mikael Sigvardsson,[10,11] and Hong Qian[1]

[1]Center for Hematology and Regenerative Medicine, Department of Medicine, Karolinska University Hospital, and [2]Division of Experimental Cancer Medicine, Department of Laboratory Medicine, Karolinska Institute, Stockholm, Sweden; [3]Clinical Research Center, Karolinska University Hospital Huddinge, Stockholm, Sweden; [4]Integrated Cardio Metabolic Centre, Department of Medicine, Karolinska University Hospital, Karolinska Institute, Stockholm, Sweden; [5]Department of Oncology and Pathology, Karolinska University Hospital, Karolinska Institute, Solna, Sweden; [6]Department of Immunology and Cell Biology, Graduate School of Biostudies, Kyoto University, Kyoto, Japan; [7]Center for Regenerative Medicine, Massachusetts General Hospital, Boston, MA; [8]Department of Stem Cell and Regenerative Biology, Harvard University, Cambridge, MA; [9]Harvard Stem Cell Institute, Cambridge, MA; [10]Department of Clinical and Experimental Medicine, Linköping University, Linköping, Sweden; and [11]Division of Molecular Hematology, Lund University, Lund, Sweden

Key Points

- *Sipa1* loss leads to BM niche alterations prior to the initiation of MPN.
- *Sipa1*-deficient BM niche induces lethal MPN from normal hematopoietic cells.

Mutations of signal-induced proliferation-associated gene 1 (*SIPA1*), a RAP1 GTPase-activating protein, were reported in patients with juvenile myelomonocytic leukemia, a childhood myelodysplastic/myeloproliferative neoplasm (MDS/MPN). *Sipa1* deficiency in mice leads to the development of age-dependent MPN. However, *Sipa1* expression in bone marrow (BM) microenvironment and its effect on the pathogenesis of MPN remain unclear. We here report that *Sipa1* is expressed in human and mouse BM stromal cells and downregulated in these cells from patients with MPN or MDS/MPN at diagnosis. By using the $Sipa1^{-/-}$ MPN mouse model, we find that *Sipa1* deletion causes phenotypic and functional alterations of BM mesenchymal stem and progenitor cells prior to the initiation of the MPN. Importantly, the altered $Sipa1^{-/-}$ BM niche is required for the development of MDS/MPN following transplantation of normal hematopoietic cells. RNA sequencing reveals an enhanced inflammatory cytokine signaling and dysregulated *Dicer1*, *Kitl*, *Angptl1*, *Cxcl12*, and *Thpo* in the $Sipa1^{-/-}$ BM cellular niches. Our data suggest that *Sipa1* expression in the BM niche is critical for maintaining BM niche homeostasis. Moreover, *Sipa1* loss–induced BM niche alterations likely enable evolution of clonal hematopoiesis to the hematological malignancies. Therefore, restoring *Sipa1* expression or modulating the altered signaling pathways involved might offer therapeutic potential for MPN.

Introduction

Normal hematopoiesis is well maintained by a rare population of hematopoietic stem cells (HSCs) residing in a specific bone marrow (BM) microenvironment, called niche.[1] The HSC fates are determined by both the extrinsic cues emanating from their niche and the intrinsic signals triggered by interactions with the niche cells via direct cell adhesion and secreted factors.[2] The BM HSC niche is composed of various types of stromal cells, including osteoblasts, adipocytes, macrophages, megakaryocytes (MKs), perivascular cells, endothelial cells, and mesenchymal stem cells (MSCs).[2,3] MSCs are considered the precursor of osteoblasts, adipocytes, and chondrocytes.[4] They can be functionally estimated by their ability to generate colony-forming unit-fibroblast (CFU-F) in vitro and are proposed to give rise to mesenchymal progenitors (MPCs) with single- or bi-lineage potential, but with no/little CFU-F activity.[3,5]

Submitted 23 October 2017; accepted 10 February 2018. DOI 10.1182/bloodadvances.2017013599.

The full-text version of this article contains a data supplement.

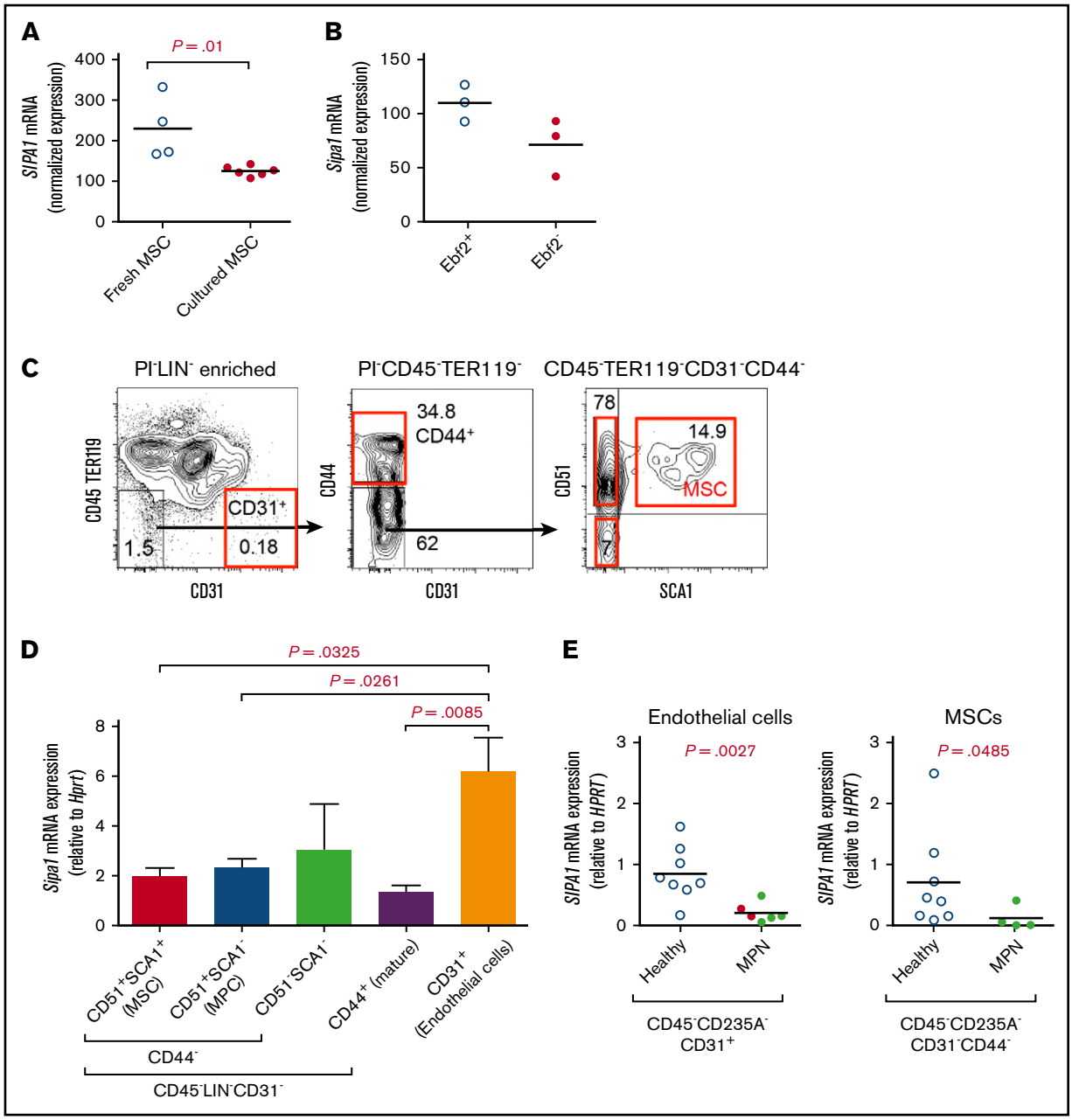

Figure 1. *Sipa1* is expressed in BM mesenchymal cells and downregulated in the stromal cells from patients with MPN. (A-B) Microarray analysis showed *SIPA1* gene expression in native and culture-expanded BM MSCs of healthy donors (A) and mice (B). The data on *SIPA1* expression in human MSCs were extracted from 2 independent experiments previously done on the freshly sorted $CD45^-CD235A^-CD31^-CD44^-$ cells and the culture-expanded MSCs. The data on *Sipa1* expression in the $Ebf2^+$ MSCs were from 3 independent experiments. The expression in mouse cells was normalized to 4 housekeeping genes, including *Gapdh*, β-*Actin*, *Transferrin Receptor*, *Pyruvate Carboxylase*, in mouse cells and to 3 housekeeping genes, including *GAPDH*, β-*Actin*, *ISGF-3* (*STAT1*), in human cells by DNA-Chip analyzer (dChip) analysis, as described.[27,28] (C) FACS profiles showing the gating strategy for sorting of $SCA1^+CD51^+$ MSCs, $SCA1^-CD51^+$ MPCs, and the more mature $SCA1^-CD51^-$ stromal cells from young adult mouse BM. The cells were first gated within $CD45^-TER119^-CD31^-CD44^-$ cells, and then the $CD31^+$ endothelial cells and the $CD44^+$ mature stromal cells were gated within the $CD45^-TER119^-$ cells as indicated. (D) qPCR analysis of *Sipa1* messenger RNA (mRNA) expression in the BM stromal cell subsets. Data are mean ± standard error of the mean (SEM), from 5 independent experiments. *Hprt* was used to normalize the expression. *P* values were calculated by unpaired Student *t* test. (E) qPCR analysis revealed downregulation of *SIPA1* expression in the BM endothelial cells and MSCs of newly diagnosed patients with CML, CNL, and CMML. *P* values between the patients and the age-matched healthy controls were tested by unpaired Mann-Whitney *U* test. *HPRT* was used to normalize the expression. Red dot indicates CMML and CNL samples.

There is increasing evidence that BM niche alterations lead to the development of myeloid malignancies.[6,7] Mice deficient for retinoic acid receptor γ developed myeloproliferative neoplasm (MPN)-like disease, which was induced solely by the gene loss in the microenvironment.[8] Deletion of *Dicer1* from mouse BM osteoblast progenitors caused myelodysplasia (MDS) that could evolve to

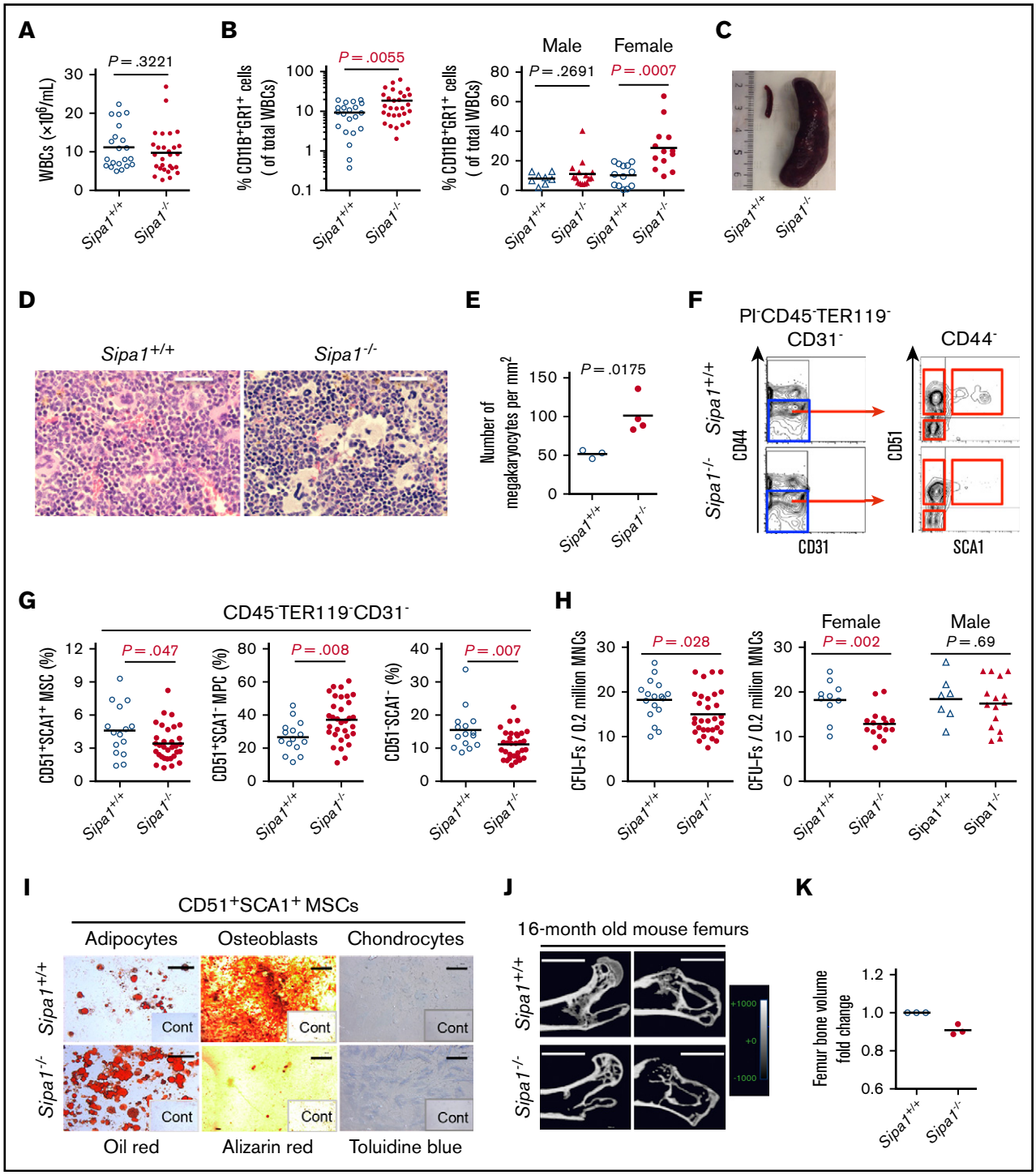

Figure 2. Myeloproliferation and altered BM niches in aged *Sipa1*$^{-/-}$ MPN mice. The PB, BM, and spleen from the age- and sex-matched aged (16-17 months old) *Sipa1*$^{+/+}$ and *Sipa1*$^{-/-}$ mice were collected for analyzing both hematopoiesis and BM niches. Statistical analysis was performed by unpaired Mann-Whitney *U* test. (A) Total white blood cells (WBCs) in 16-month-old *Sipa1*$^{+/+}$ and *Sipa1*$^{-/-}$ mice. (B) Myeloid cells in the PB of the *Sipa1*$^{+/+}$ and *Sipa1*$^{-/-}$ male and female mice. (C) A representative splenomegaly (right) of the aged *Sipa*1$^{-/-}$ mice. (D) Hematoxylin and eosin (H&E) staining of dysplastic MKs in the *Sipa1*$^{-/-}$ mouse BM. Scale bars represent 50 μm. (E) The increased numbers of MKs in the *Sipa1*$^{-/-}$ mouse BM. The data are expressed as numbers per squared millimeters. (F) FACS profiles for phenotypic analysis of BM stromal cells in the *Sipa1*$^{+/+}$ and *Sipa1*$^{-/-}$ mice. The CD44^{-} cells were first gated within CD45^{-}TER119^{-}CD31^{-} cells and then subdivided into SCA1^{+}CD51^{+} MSCs, SCA1^{-}CD51^{+} MPCs, and SCA1^{-}CD51^{-} mature stromal cells. (G) Altered stromal cell composition in the BM of 16-month-old *Sipa1*$^{-/-}$ mice. Data are percent of the cells within total CD45^{-}TER119^{-}CD31^{-} cells from 8 independent experiments. (H) CFU-F frequencies in whole BM cells. The right panel shows the difference in the frequencies of CFU-Fs observed between the female or male *Sipa1*$^{+/+}$ and *Sipa1*$^{-/-}$ mice. (I) Multilineage differentiation potentials of the *Sipa1*$^{-/-}$ BM MSCs. Scale bars represent 250 μm (left), 500 μm (middle), and 100 μm (right). n = 3 independent sorting experiments. (J) μCT images of femurs in the aged *Sipa1*$^{+/+}$ and *Sipa1*$^{-/-}$ female mice. Scale bars represent 1.0 mm. (K) Femoral bone volumes of *Sipa1*$^{+/+}$ and *Sipa1*$^{-/-}$ mice. The statistical difference was determined by Mann-Whitney *U* test (A) or unpaired Student *t* test (B-E, G-H). See also supplemental Figure 1. Cont, control.

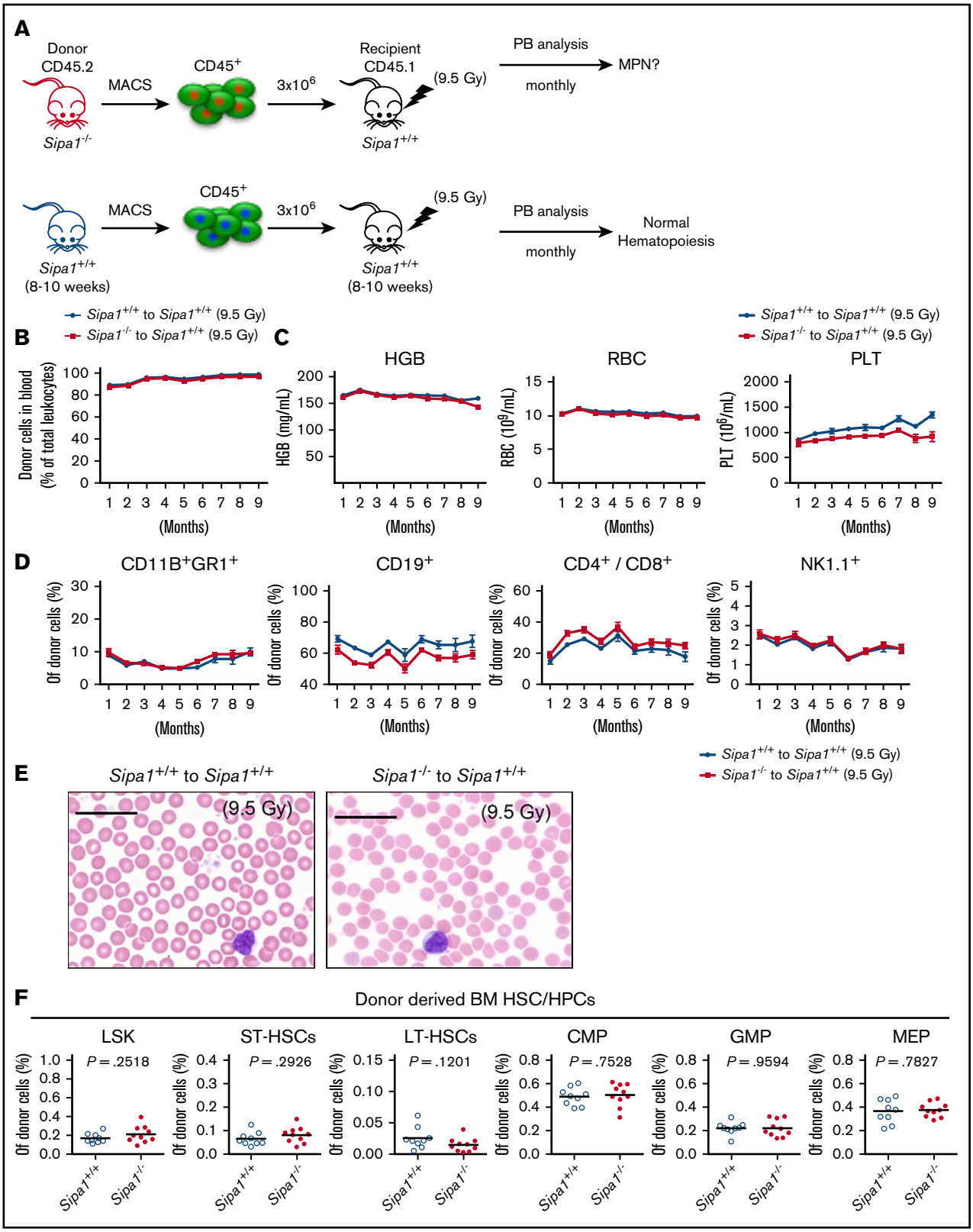

Figure 3. *Sipa1*$^{-/-}$ hematopoietic cells failed to develop any hematological disorders after transplantation into young *Sipa1*$^{+/+}$ mice. (A) Transplantation setup. The CD45.2^{+} cells from 8- to 10-week-old *Sipa1*$^{+/+}$ or *Sipa1*$^{-/-}$ mouse BM were transplanted into lethally irradiated CD45.1 *Sipa1*$^{+/+}$ recipient mice (8-10 weeks old). Donor-derived lineages in the PB were analyzed by FACS monthly after transplantation. (B) Total donor engraftment in the recipient PB. (C) Red blood cells (RBC), hemoglobin (HGB), and platelets (PLT) in the recipient PB. (D) FACS analysis of blood lineage reconstitution after transplantation.

acute myeloid leukemia (AML).[9] In addition, loss of Notch signaling in the BM niche led to lethal MPN-like disease.[10] A recent study revealed the critical contribution of *Ptpn11* mutations in BM MPCs to leukemogenesis.[11]

Signal-induced proliferation-associated gene 1 (Sipa1), a principal RAP1 GTPase-activating protein, regulates signaling of integrins, growth factors, and cytokines by inactivating RAP1.[12-14] *Sipa1* is expressed in mouse hematopoietic stem and progenitor cells (HSPCs) and human lymphocytes.[15,16] Loss of *Sipa1* leads to constitutive hyperactivation of RAP1, cell proliferation, and development of malignancy.[14,17,18] Mutations or abnormal expression of *SIPA1* have been reported in hematopoietic malignancies and solid cancer in humans.[19-21] *SIPA1* gene point mutations were identified in patient mononuclear cells with juvenile myelomonocytic leukemia,[22] a childhood MDS/MPN,[23] and AML.[24] *Sipa1*$^{-/-}$ mice show normal hematopoiesis at a younger age (before 5 months), but develop MPN, resembling human chronic myeloid leukemia (CML) or MDS, from 1 year of age.[15,25] However, it is unclear whether the MPN is caused by *Sipa1* loss in hematopoietic cells or in BM stromal cells.

We here report that *Sipa1* is expressed in BM stromal cells and downregulated in these cells from patients with MPN or MDS/MPN. *Sipa1* deficiency in mice induces significant alterations in the BM niche prior to the initiation of MDS/MPN. Importantly, the altered *Sipa1*$^{-/-}$ BM microenvironment is absolutely required for the MDS/MPN development in the *Sipa1*$^{-/-}$ mice. *Sipa1* loss confers greater capacity on BM MSCs and MPCs to promote myelopoiesis. The dysregulated cytokine signaling in the *Sipa1*$^{-/-}$ BM niche may be involved in the pathogenesis of the disease.

Materials and methods

Mice

Sipa1$^{-/-}$ C57BL/6 mice[15] were backcrossed to C57BL/6 for >15 generations. The *Sipa1*$^{-/-}$ mice at 8 to 12 weeks and 16 to 17 months were used for experiments. Age- and sex-matched *Sipa1*$^{+/+}$ C57BL/6 mice were used as controls. CD45.1 B6.SJL-Ptprca Pepcb/BoyJ (Jackson Laboratory, Bar Harbor, ME) mice were used as recipients or donors for transplantations. All the mice were maintained in a specific pathogen-free condition in the animal facility at Karolinska Institute. Animal procedures were performed with approval from the local ethics committee (ethical number S40-14) at Karolinska Institute (Stockholm, Sweden).

Human sample collection

BM samples were collected from patients (49-78 years old) with CML, chronic neutrophilic leukemia (CNL), or chronic myelomonocytic leukemia (CMML), classified as MPN and MDS/MPN,[23,26] at diagnosis and from the age-matched (45-86 years old) healthy donors. The experiments were approved by the local Ethical Committee at Stockholm (2012/4:10 and 2013/3:1) and informed consent was obtained from the patients and healthy donors.

Multicolor fluorescence activated cell sorting (FACS) of MSCs

Human and mouse MSCs were isolated as described.[27,28] See supplemental Data for details.

CFU-F assay

CFU-F assay of freshly sorted BM MSCs or unfractionated cells was performed as described.[27,28]

Transplantations

BM cells from 7- to 10-week-old *Sipa1*$^{+/+}$ (CD45.1^{+} or CD45.2^{+}) or *Sipa1*$^{-/-}$ (CD45.2^{+}) mice were enriched by magnetic-activated cell sorting using CD45 microbeads (Miltenyi Biotec). Three million of the cells per mouse were injected via tail vein into sublethally (6 Gy) or lethally (9.5 Gy) irradiated young (8- to 10-week-old) CD45.2 *Sipa1*$^{-/-}$ and *Sipa1*$^{+/+}$ recipient mice. When transplanting the *Sipa1*$^{-/-}$ cells, 8- to 10-week-old CD45.1 *Sipa1*$^{+/+}$ mice (lethally irradiated) were used as recipients. At the endpoints (7-9 months) of the primary transplantations, 3 million spleen cells from the primary *Sipa1*$^{-/-}$ recipients (CD45.2), which had developed MDS/MPN, were transplanted into sublethally irradiated *Sipa1*$^{+/+}$ recipients (CD45.2). The analysis of hematopoiesis after transplantation is described in supplemental Data.

RNA sequencing

Total RNA was isolated from sorted cells, and libraries were constructed using NuGEN's Ovation Ultralow Library systems (NuGEN Technologies, San Carlos, CA) and were subsequently subjected to 50 cycles of HiSequation 2000 or 76 cycles of NextSeq500 sequencing (Illumina, San Diego, CA). See supplemental Data for more details and data analysis.

Statistics

The unpaired Student *t* test or Mann-Whitney *U* test, Welch's correction, and Kolmogorov-Smirnov test were used to compare the differences based on the data distribution. The Kaplan-Meier survival curve of the mice was generated by Prism 6.0. All reported *P* values were obtained using Prism 5.0 or 6.0, and $P < .05$ was considered statistically significant.

See additional methods in supplemental Data.

Results

Sipa1 is expressed in normal BM stromal cells and downregulated in patients with MPN

Previous studies have shown that *Sipa1* was expressed in hematopoietic progenitors and lymphoid cells.[15,16] *Sipa1* expression in BM nonhematopoietic cells is unclear. Analysis of the microarray data from our previous studies[28,29] revealed that *SIPA1* was also expressed in human BM MSCs, and mouse BM MSCs expressing

Figure 3. (continued) The data are mean ± SEM, from 2 independent experiments, n = 9 to 10 per group. (E) H&E staining of PB smears of the *Sipa1*$^{+/+}$ recipients 9 months after transplantation of donor *Sipa1*$^{-/-}$ or *Sipa1*$^{+/+}$ BM CD45.2^{+} cells. Scale bars represent 25 μm. (F) Reconstitution of HSPCs in the recipient BM 9 months after transplantation. CMP, common myeloid progenitor; LT-HSCs, long-term HSCs; ST-HSCs, short-term HSCs.

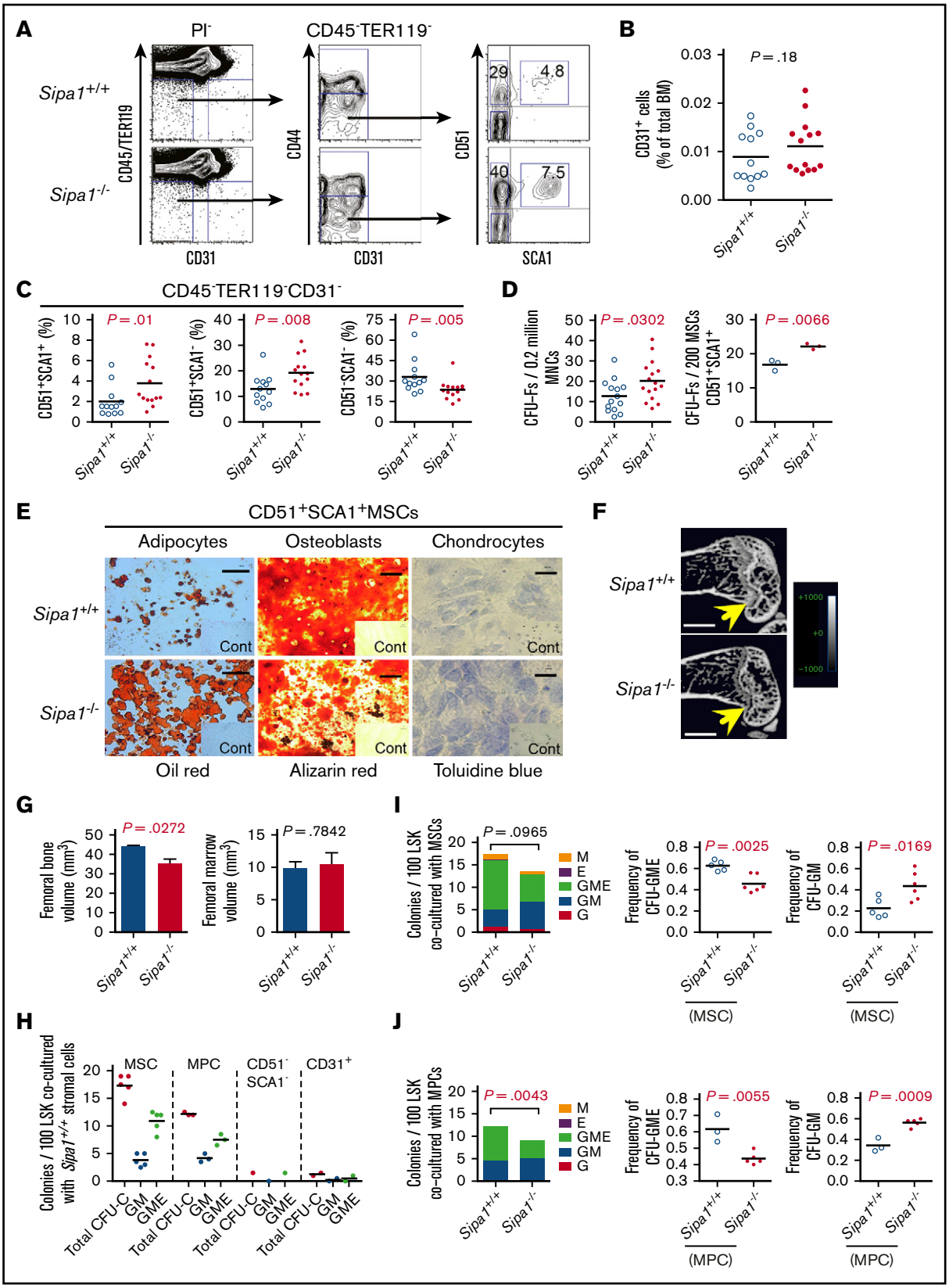

Figure 4. Phenotypic and functional alterations of BM mesenchymal cells in the *Sipa1*$^{-/-}$ mice prior to the initiation of MPN. (A) Representative FACS profiles of the analysis of BM stromal cells subsets in 3-month-old *Sipa1*$^{+/+}$ and *Sipa1*$^{-/-}$ mice. The CD45$^-$TER119$^-$CD31$^-$PI$^-$ cells were first divided into the CD44$^-$ and CD44$^+$ cells. The SCA1$^+$CD51$^+$ MSCs, SCA1$^+$CD51$^-$ MPCs, and SCA1$^-$CD51$^-$ cells were subsequently gated within the CD44$^-$ cells. (B) The frequency of CD31$^+$ cells in the

early B-cell factor 2 (Ebf2)[27] (Figure 1A-B), a recently identified MSC population[27] that is partly overlapping with the Nestin$^+$ MSCs.[30] To further determine the *Sipa1* gene expression in different mouse BM stromal cell fractions, we performed quantitative real-time polymerase chain reaction (qPCR) analysis on FACS-sorted BM endothelial cells (CD45$^-$LIN$^-$CD31$^+$), MSCs (CD45$^-$LIN$^-$CD31$^-$CD44$^-$CD51$^+$SCA1$^+$),[28,29] and MPCs (CD45$^-$LIN$^-$CD31$^-$CD44$^-$CD51$^+$SCA1$^-$), which contain most of the CXCL12-abundant cells.[5,31] We detected *Sipa1* gene expression in all the stromal cell subsets, with the highest *Sipa1* expression in the endothelial cells (Figure 1C-D). Interestingly, *SIPA1* expression was significantly reduced in BM endothelial cells ($P = .0027$) of patients with CML, CNL, or CMML compared with age-matched controls, and to a lesser extent reduced in the MSCs (Figure 1E).

Altered BM niche in aged *Sipa1*$^{-/-}$ mice after the development of MDS/MPN

To investigate the contribution of the BM niche to the development of MDS/MPN, we characterized the BM niche in the 16-month-old *Sipa1*$^{-/-}$ mice. Consistent with the previous report,[15] the majority of the *Sipa1*$^{-/-}$ mice developed MDS-like MPN, which can be categorized as MDS/MPN.[32] The disease was manifested by anemia, thrombocytopenia, increased granulocytes, pronounced B-lymphopenia, and splenomegaly (occurring in ~28.6% of the female mice) (Figure 2A-C; supplemental Figure 1), macrocytic erythrocytes, and increased neutrophils in the peripheral blood (PB) (supplemental Figure 1D-E). We also observed an increased leukocyte infiltration concomitant with MK hyperplasia in the *Sipa1*$^{-/-}$ BM (Figure 2D-E). The hyperplastic MK formed many loose clusters and showed smaller hypolobated, pyknotic, or fragmented nuclei and abnormal cytoplasmic morphology. There is a gender bias of the disorders toward the female *Sipa1*$^{-/-}$ mice (Figure 2B; supplemental Figure 1A-C).

To explore any potential BM stromal cell alterations in these mice, we dissected the BM stromal cell compartment by FACS. The frequencies of the MSCs and the mature stromal cells were significantly reduced, whereas the MPCs were increased in the aged *Sipa1*$^{-/-}$ mice (Figure 2F-G). The reduction of the MSCs was confirmed by the decreased number of CFU-Fs, reflecting the functionally defined MSCs, in *Sipa1*$^{-/-}$ mouse BM (Figure 2H left). Consistent with the observation of a female bias of the MDS/MPN, the reduced CFU-F activities were mainly detected in the MSCs from the *Sipa1*$^{-/-}$ female mice (Figure 2H right). The frequencies of the endothelial cells remained unchanged (data not shown). Moreover, the *Sipa1*$^{-/-}$ MSCs showed increased adipogenic and chondrogenic, but impaired osteogenic differentiation potential (Figure 2I). Micro-computed tomography (μCT) showed slightly reduced femoral bone volume in the aged *Sipa1*$^{-/-}$ mice (Figure 2J-K). These data suggest phenotypic and functional alterations of BM cellular niches in the aged *Sipa1*$^{-/-}$ mice with MDS/MPN.

The development of MPN in aged *Sipa1* $^{-/-}$ mice is not dependent on intrinsic loss of *Sipa1* in hematopoietic cells

The discovery of *Sipa1* expression in the BM stromal cells and the BM niche alterations in the aged *Sipa1*$^{-/-}$ mice raised a question of whether the MDS/MPN in the aged *Sipa1*$^{-/-}$ mice was attributable to the *Sipa1* deletion from the BM stromal cells. To answer this question, we transplanted BM hematopoietic cells from young adult *Sipa1*$^{-/-}$ mice into lethally irradiated wild-type mice (Figure 3A). Surprisingly, we could not detect any signs of hematological disorders (Figure 3). These data clearly suggest that the loss of *Sipa1* in the hematopoietic cells is not sufficient to initiate the MPN.

Loss of *Sipa1* results in alterations of BM niche prior to the initiation of MDS/MPN

The absence of MPN after transplantation of *Sipa1*$^{-/-}$ hematopoietic cells into a wild-type environment pointed to the potential critical contribution of the *Sipa1*$^{-/-}$ BM niche to the MPN. To test this, we analyzed the BM cellular niche components in young (2-3 months old) *Sipa1*$^{-/-}$ mice where no abnormal hematopoiesis was observed (supplemental Figure 2). FACS analysis indicated that both MSCs and MPCs, but not CD31$^+$ cells, were significantly expanded in the young *Sipa1*$^{-/-}$ BM (Figure 4A-C). Correspondingly, the CFU-F frequencies in the unfractionated BM cells and the sorted MSCs from the *Sipa1*$^{-/-}$ mice were increased (Figure 4D). The *Sipa1*$^{-/-}$ MSCs displayed increased adipogenic, but reduced osteogenic differentiation potential (Figure 4E). μCT analysis revealed a reduced femoral bone volume (Figure 4F-G left) in the young *Sipa1*$^{-/-}$ mice compared with that in the age-matched *Sipa1*$^{+/+}$ mice, supporting the finding of impaired osteoblast differentiation capacity of the *Sipa1*$^{-/-}$ MSCs.

To evaluate the hematopoiesis-supportive function of different *Sipa1*$^{-/-}$ MSCs, MPCs, and endothelial cells, we cocultured these sorted cells with normal Lin$^-$SCA1^{high}KIT^{high} (LSK) HSPCs (Figure 4H-J). *Sipa1*$^{-/-}$ MSCs and MPCs displayed significantly stronger capacity in promoting myeloid cell differentiation, indicated by more granulocyte-macrophage (GM) colonies, but less multilineage (GM and erythrocyte, GME) colonies generated in the cultures with the *Sipa1*$^{-/-}$ stromal cells compared with that with *Sipa1*$^{+/+}$ stromal cell counterparts (Figure 4I-J).

Taken together, these data demonstrated the dramatic alterations in composition and function of the BM niche in young *Sipa1*$^{-/-}$ mice prior to the onset of the MDS/MPN.

Figure 4. (continued) *Sipa1*$^{+/+}$ and *Sipa1*$^{-/-}$ mouse BM. (C) The percent of the MSCs, MPCs, and the SCA1$^-$CD51$^-$ cells within total CD45$^-$TER119$^-$CD31$^-$ stromal cells. The data are from 3 independent experiments. (D) CFU-F frequencies in *Sipa1*$^{+/+}$ and *Sipa1*$^{-/-}$ mouse BM MNCs and FACS-sorted MSCs. (E) Multilineage differentiation potentials of MSCs from *Sipa1*$^{+/+}$ and *Sipa1*$^{-/-}$ BM. Scale bars represent 250 μm (left), 500 μm (middle), and 50 μm (right). n = 3 independent sorting experiments. (F) Representative μCT images of the longitudinal femoral section indicating reduced bone mass of *Sipa1*$^{-/-}$ mouse femurs. Scale bars represent 1.0 mm. (G) Femoral bone (left) and marrow (right) volumes of *Sipa1*$^{+/+}$ and *Sipa1*$^{-/-}$ mice. n = 3 per group of each genotype. (H) Colony-forming unit in culture (CFU-C) colonies derived from 100 LSK cells cocultured with *Sipa1*$^{+/+}$ BM MSC, MPC, CD51$^-$SCA1$^-$ mature stromal cells and endothelial cells. Total CFU-C, colonies with GM, G, M, erythrocytes (E), and GME lineages were counted. (I-J) The numbers of CFU-C colonies per 100 LSK cells after coculture with *Sipa1*$^{+/+}$ and *Sipa1*$^{-/-}$ MSC (I) and MPC (J). Data were collected from 2 to 3 independent experiments. The statistical difference was determined by unpaired Student *t* test. See also in supplemental Figure 2.

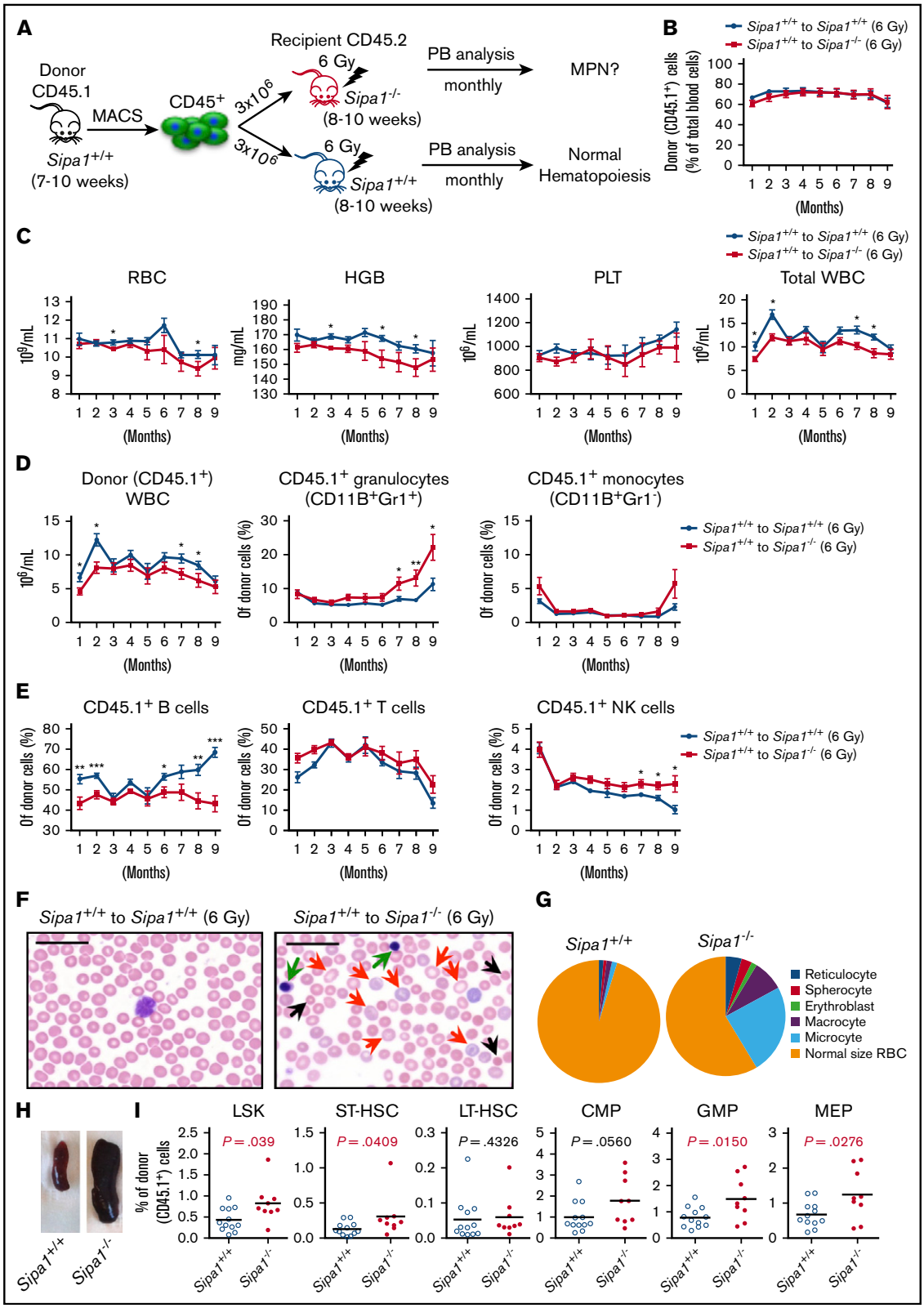

Figure 5. *Sipa1*$^{-/-}$ niche induces MDS/MPN from normal hematopoietic cells after transplantation following sublethal irradiation. (A) Experimental design, normal hematopoietic cells. Three million normal BM CD45.1^{+} cells from a 7- to 10-week-old *Sipa1*$^{+/+}$ mouse were sorted by magnetic-activated cell sorting (MACS) and transplanted into sublethally irradiated CD45.2^{+} young (8-10 week old) *Sipa1*$^{+/+}$ and *Sipa1*$^{-/-}$ recipient mice. The PB of the recipients was monitored monthly after transplantation. (B) Total donor-derived blood reconstitution in the *Sipa1*$^{+/+}$ and *Sipa1*$^{-/-}$ recipients after transplantation. Data are mean ± SEM, from 2 independent

Sipa1-deficient BM niche induces myeloproliferation and erythrocyte dysplasia after transplantation

To determine the role of the altered BM niche in the young *Sipa1*$^{-/-}$ mice for the initiation of the MPN, we next transplanted the *Sipa1*$^{+/+}$ BM hematopoietic cells into sublethally (6 Gy) irradiated *Sipa1*$^{+/+}$ and *Sipa1*$^{-/-}$ recipients (Figure 5A). To avoid introducing donor BM stromal cells, we purified the CD45.1^{+} hematopoietic cells for the transplantation. About 60% to 70% donor-cell engraftment in the PB was achieved in both groups after transplantation (Figure 5B). However, we detected lower WBC, RBC, and hemoglobin counts in the *Sipa1*$^{-/-}$ recipient PB compared with that in the *Sipa1*$^{+/+}$ recipients (Figure 5C), indicating ineffective hematopoiesis of the donor cells in the *Sipa1*$^{-/-}$ niche. The donor-derived CD11B^{+}GR1^{+} granulocytes were increased at ~7 months after transplantation, whereas the CD19^{+} B cells, but not T cells, were reduced in the *Sipa1*$^{-/-}$ recipients compared with that in the *Sipa1*$^{+/+}$ recipients (Figure 5D-E). The natural killer cells were also significantly increased after transplantation in the *Sipa1*$^{-/-}$ recipient PB (Figure 5E). Moreover, PB smears of the *Sipa1*$^{-/-}$ recipients showed the presence of erythroblasts, reticular erythrocytes, spherocytes, macrocytes, and microcytes in the *Sipa1*$^{-/-}$ recipients (Figure 5F-G), supporting the notion of the dyserythropoiesis. In addition, we observed splenomegaly in 10% of the *Sipa1*$^{-/-}$ recipients 9 months after transplantation (Figure 5H). The increased myeloid cells, but decreased B cells, were also detected in the *Sipa1*$^{-/-}$ recipient BM (supplemental Figure 3A-B). Importantly, we did not observe any significant difference in host-derived hematopoietic lineage distribution between the *Sipa1*$^{+/+}$ and *Sipa1*$^{-/-}$ recipients (supplemental Figure 3B), emphasizing little contribution of the host *Sipa1*$^{-/-}$ hematopoietic cells to the MDS/MPN.

Expansion of HSPCs is a common phenotype of MPN.[33,34] The frequencies of donor-derived LSK, short-term–HSC (LSKCD34^{+}FLT3^{-}), granulocyte-macrophage progenitor (GMP; LIN^{-}SCA1^{-}KIT^{+}CD34^{high}FcγR^{high}), and MK-erythrocyte progenitor (MEP; LIN^{-}SCA1^{-}KIT^{+}CD34^{-}FcγR^{-}) were increased in the *Sipa1*$^{-/-}$ recipient BM 9 months after transplantation (Figure 5I). Meanwhile, the accumulations of CMPs and GMPs were also detected in the *Sipa1*$^{-/-}$ recipient spleen (supplemental Figure 3C). However, the frequency of host-derived HSPCs in the *Sipa1*$^{-/-}$ recipient spleen remained similar to that in the *Sipa1*$^{+/+}$ recipients (supplemental Figure 3D).

Taken together, transplantation of normal hematopoietic cells into the *Sipa1*$^{-/-}$ niche resulted in myeloproliferation along with dysplastic erythropoiesis and leukopenia, which resembles the clinic features of the overlapping syndromes of the unclassifiable MDS/MPN[35] and is consistent with MDS/MPN in mice according to the Bethesda criteria[32] and the World Health Organization classification.[36]

Neoplastic transformation of normal hematopoietic cells after transplantation into *Sipa1*$^{-/-}$ niche

To further determine the contribution of the altered *Sipa1*$^{-/-}$ niche to the initiation of MDS/MPN and the underlying molecular mechanisms, we examined the hematopoietic activity of normal BM CD45.1^{+} cells after transplantation into lethally irradiated (9.5 Gy) *Sipa1*$^{-/-}$ CD45.2^{+} mice. About 98% donor-cell engraftment was obtained in the recipients after transplantation (supplemental Figure 4A). We observed even more severe phenotype of MDS/MPN in these *Sipa1*$^{-/-}$ recipients compared with that in the sublethally irradiated recipients, which might be due to the stronger inflammatory response following lethal irradiation. The *Sipa1*$^{-/-}$ recipients exhibited reduced survival (Figure 6A), myeloproliferation accompanied with B-cell reduction (supplemental Figure 4B-C), BM hypercellularity (Figure 6B-C), and MK hyperplasia (Figure 6D-E), a characteristic feature of malignant or clonal hematological disorders.[37] The frequency of the donor-derived MEPs was increased in the *Sipa1*$^{-/-}$ recipient BM compared with that in the *Sipa1*$^{+/+}$ BM (Figure 6F). One of the *Sipa1*$^{-/-}$ recipients displayed enlarged lymph nodes (supplemental Figure 4E). Similar to what we observed in the aged *Sipa1*$^{-/-}$ mice (Figure 2C), ~28.6% (2/7) of the *Sipa1*$^{-/-}$ recipients developed splenomegaly 7 to 9 months after transplantation. H&E staining illustrated reduced lymphocytic component of white pulp in the *Sipa1*$^{-/-}$ recipient spleen (Figure 6G). This was associated with the increased frequencies of CMP, GMP, and MEP in the *Sipa1*$^{-/-}$ recipient spleen (Figure 6H-I). The malignant transformation of the normal donor cells in the *Sipa1*$^{-/-}$ recipients was indicated by the development of MDS in ~75% of the secondary recipients after receiving the spleen cells from the primary *Sipa1*$^{-/-}$ recipients with MDS/MPN. The secondary recipients exhibited increased mortality, anemia, thrombocytopenia, and splenomegaly 6 months after the transplantation (Figure 6J-K). To explore the molecular mechanisms underlying the pathogenesis of the disease, we performed whole-exome sequencing of the donor cells sorted from *Sipa1*$^{-/-}$ and *Sipa1*$^{+/+}$ primary recipients. However, we only detected a few genetic variants in the donor cells from *Sipa1*$^{-/-}$ BM and spleen in 1 of the experiments (data are not shown).

Dysregulated inflammatory cytokines and growth factors in the *Sipa1*$^{-/-}$ BM stromal cells

To investigate the molecular mechanisms underlying the niche-induced MDS/MPN, we performed RNA sequencing on the native BM MSCs, MPCs, and endothelial cells from young (8-10 week old) *Sipa1*$^{-/-}$ and *Sipa1*$^{+/+}$ mice. As expected, gene set enrichment analysis showed that G-protein signal pathways, including *Ras* and *Rap1* signaling, were elevated in the *Sipa1*$^{-/-}$ MSCs and endothelial cells (supplemental Figures 5A-B and 6). Proinflammatory cytokines,

Figure 5. (continued) experiments, n = 12 *Sipa1*$^{+/+}$ recipients and n = 10 *Sipa1*$^{-/-}$ recipients. (C) RBCs, HGB, PLTs, and total WBCs in the recipient PB. The PB was analyzed monthly for monitoring the development of the disorders in the PB of the sublethally irradiated *Sipa1*$^{+/+}$ and *Sipa1*$^{-/-}$ recipients after transplantation. (D) Donor-derived WBC and myeloid cells in *Sipa1*$^{+/+}$ and *Sipa1*$^{-/-}$ mice after transplantation. (E) Donor-derived B cells, T cells, and natural killer cells in the *Sipa1*$^{+/+}$ and *Sipa1*$^{-/-}$ mice after transplantation. (F) H&E staining of PB smears of the *Sipa1*$^{+/+}$ and *Sipa1*$^{-/-}$ recipients 9 months after transplantation. Scale bars represent 25 μm. Black arrows indicate microcytes; red arrows indicate macrocytes, and green arrows indicate erythroblasts, respectively. (G) Distribution of reticulocytes, macrocytes, microcytes, spherocytes, erythroblasts, and normal size RBC. (H) Splenomegaly in the *Sipa1*$^{-/-}$ recipients 6 to 9 months after transplantation. (I) Enhanced expansion of donor-derived HSPCs in the recipient *Sipa1*$^{-/-}$ BM 9 months after transplantation. The donor-derived (CD45.1^{+}) HSCs and HPCs were calculated in total BM Lineage (LIN)$^{-}$ cells. $^{*}P < .05$; $^{**}P < .01$; $^{***}P < .001$, analyzed by unpaired Mann-Whitney *U* test. See also in supplemental Figure 3.

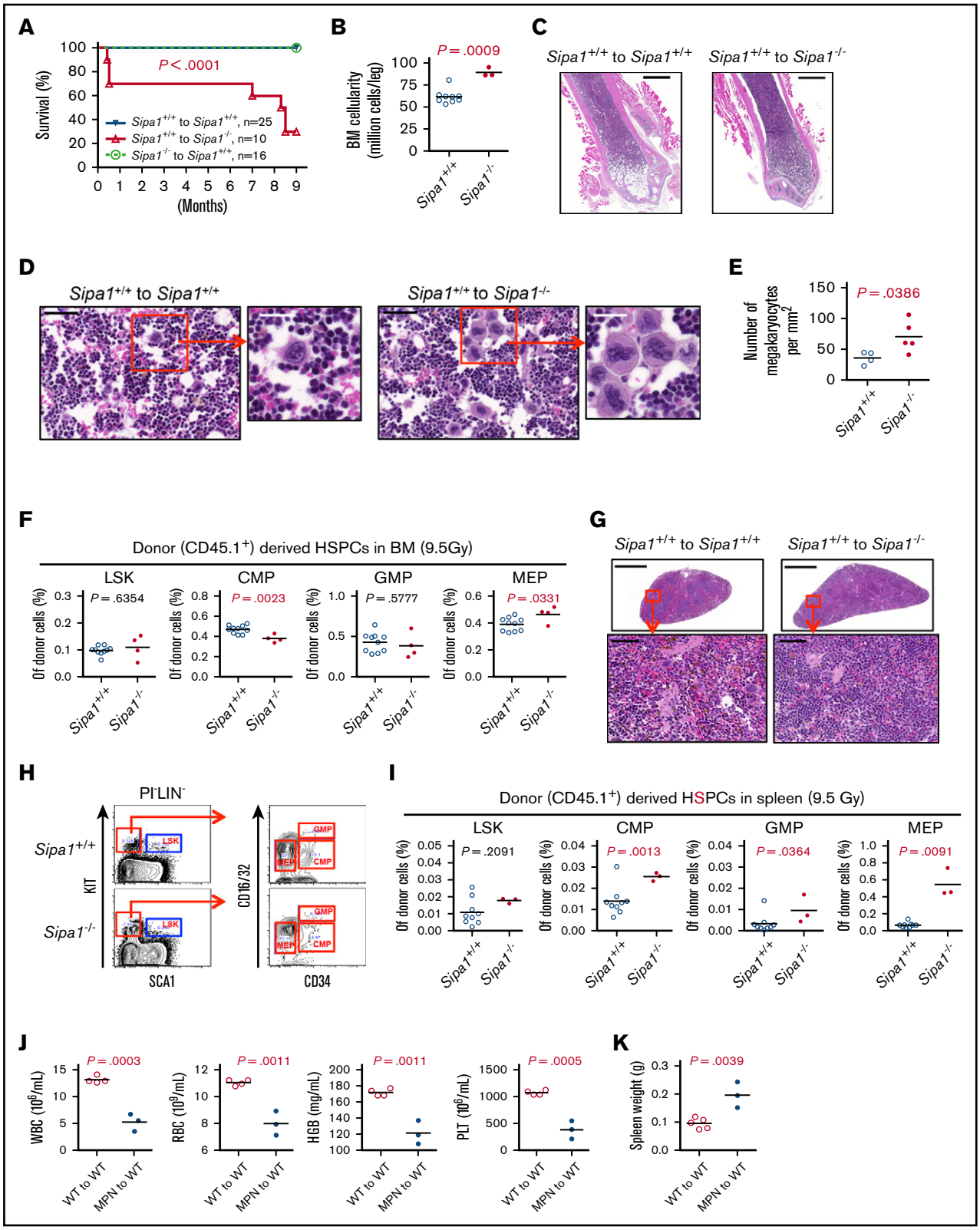

Figure 6. Development of lethal MDS/MPN in the lethally irradiated *Sipa1*$^{-/-}$ recipients. Three million normal BM CD45.1^{+} cells from 8- to 9-week-old *Sipa1*$^{+/+}$ mice were transplanted into lethally irradiated CD45.2^{+} young (8-10 week old) *Sipa1*$^{+/+}$ and *Sipa1*$^{-/-}$ recipient mice. (A) Kaplan-Meier survival curves of the lethally irradiated *Sipa1*$^{+/+}$ and *Sipa1*$^{-/-}$ recipients after transplantation. The statistic difference was determined by Logrank Mantel Cox test. (B) The total BM cellularity 9 months after the transplantation. (C) Representative H&E-stained femoral sections showed increased leukocytes infiltration in the BM from the *Sipa1*$^{-/-}$ recipients. Scale bars represent

including transforming growth factor-β (TGF-β) and the IL6/JAK/STAT3 signaling pathways, were significantly increased in the *Sipa1*$^{-/-}$ MSCs (Figure 7A). Similarly, *Il4* and *Mapk* in the FcεRI-mediated signaling pathway were also elevated in the *Sipa1*$^{-/-}$ MPCs (supplemental Figure 5C). Within the top 25 changed genes in the *Sipa1*$^{-/-}$ MPCs, thrombopoietin (*Thpo*), a growth factor critical for HSC maintenance and the development of MPN, was increased in the *Sipa1*$^{-/-}$ MPCs (Figure 7B). The TGF-β and tumor necrosis factor-α (TNF-α) signaling pathways were also enhanced in the *Sipa1*$^{-/-}$ endothelial cells (Figure 7C). In addition, the extracellular matrix receptor interactions, wingless-type MMTV integration site family β (WNT-β) catenin, interleukin-2 (IL-2), β-catenin (*Ctnnb1*), and Notch signaling were enriched in the *Sipa1*$^{-/-}$ endothelial cells (supplemental Figure 5D-E).

Consistent with the impaired osteogenic differentiation potential of the *Sipa1*$^{-/-}$ MSCs, the expression of runt-related transcription factor 2 (*Runx2*), a master gene for osteoblast differentiation, was reduced in the *Sipa1*$^{-/-}$ MSCs and MPCs (Figure 7D-E). Furthermore, expression of the lymphopoiesis-promoting cytokine *Il7* and *Dicer1*, a microRNA-processing gene, was reduced in the *Sipa1*$^{-/-}$ MPCs (Figure 7E).

Cxcl12, *Kitl*, and *Angptl1* are known to be critical for maintaining HSC quiescence.[38-42] The significant downregulations of *Cxcl12*, *Kitl*, and *Angptl1* were observed in *Sipa1*$^{-/-}$ BM MSCs and MPCs, but not in endothelial cells (Figure 7D-F) compared with the *Sipa1*$^{+/+}$ cell counterparts. However, erythropoietin (*Epo*) expression in the *Sipa1*$^{-/-}$ endothelial cells was increased (Figure 7G). Together, these data indicate that *Sipa1* loss in BM stromal cells causes molecular alteration of the niche factors that may contribute to the pathogenesis of MPN.

Discussion

Recent studies have reported that genetic alterations of BM stromal cells can be involved in the pathogenesis of MPN and AML.[2,11] However, the cellular and molecular mechanisms underlying the microenvironment-induced leukemogenesis remain poorly understood. We here demonstrate that *Sipa1* deletion results in BM niche alterations leading to the development of MDS/MPN.[32,35] The initiation of the MDS/MPN in this model is dependent on the altered BM niche resulting from the *Sipa1* deficiency in BM microenvironment, not in hematopoietic cells. The dysregulated inflammatory cytokines in *Sipa1*-deficient niche might contribute to the pathogenesis of MDS/MPN.

SIPA1 is a G-protein signaling component of many growth factors and cytokine, including IL-3, granulocyte-macrophage colony-stimulating factor, and CXCL12 in hematopoietic cells.[12-14] *SIPA1* point mutations were detected in mononuclear cells of patients with juvenile myelomonocytic leukemia but lacking detectable mutations of other G-protein signaling molecules *KRAS*, *NRAS*, and *PTPN11*.[22] However, the cell origin of the mutation remains unclear. Previous studies showed that the majority of the *Sipa1*$^{-/-}$ mice and 15% *Sipa1*$^{+/-}$ mice developed CML-like MPN.[15,25] We here observed MDS-like MPN mainly in the aged *Sipa1*$^{-/-}$ female mice. This discrepancy in the observed disease phenotype might be due to different genetic background of the mice. The female-biased development of the MDS/MPN could be attributed to the declined bone-forming ability in the aged female mice,[43,44] which could deteriorate the phenotype of the impaired osteoblast differentiation induced by *Sipa1* deletion. Nevertheless, the impact of *Sipa1* deletion in BM microenvironment on the MDS/MPN remains unexplored.

We here for the first time report *SIPA1* expression in human and mouse native BM stromal cells. The importance of Sipa1 expression in BM niche is supported by the abnormal expansion and differentiation of MSCs and MPCs in young *Sipa1*$^{-/-}$ mouse BM prior to the initiation of the MDS/MPN, which could contribute to the pathogenesis of the disease. Furthermore, the *SIPA1* gene is downregulated in BM MSCs and endothelial cells from patients with CML, CMML, and CNL. This finding merits future study on the impact of *SIPA1* gene alteration in BM niche on the treatment outcome in patients with MPN, particularly in the patients who undergo allogenic stem cell transplantation.

The absolute requirement of *Sipa1*$^{-/-}$ BM niche for the generation of the MPN in the *Sipa1*$^{-/-}$ aged mice is demonstrated by the reciprocal transplantation of normal *Sipa1*$^{+/+}$ hematopoietic cells into irradiated *Sipa1*$^{-/-}$ and *Sipa1*$^{+/+}$ mice, or vice versa. The sustained normal hematopoiesis after transplantation of *Sipa1*$^{-/-}$ hematopoietic cells in normal microenvironment suggests that the intrinsic loss of *Sipa1* gene in hematopoietic cells is not sufficient to induce the MPN. In contrast, the *Sipa1*$^{-/-}$ recipients developed lethal MDS/MPN after transplantation of *Sipa1*$^{+/+}$ hematopoietic cells. The features of the disease in the *Sipa1*$^{-/-}$ recipients almost completely recapitulated the MDS/MPN in the aged *Sipa1*$^{-/-}$ mice. Our data suggest that the MDS/MPN in the aged *Sipa1*$^{-/-}$ mice is actually driven by the BM niche, not the *Sipa1* deletion in hematopoietic cells. This finding is in contrast to the previous report that *Sipa1*$^{-/-}$ hematopoietic cells from the mice with established MPN continued developing CML-like disease after transplantation.[15] This discrepancy could be mainly due to the fact that the donor *Sipa1*$^{-/-}$ cells in the previous study were already transformed to be leukemic, and thus, might have developed niche independence, as reported.[45] Therefore, it is critical that we transplanted *Sipa1*$^{-/-}$ hematopoietic cells from young adult mice where hematopoiesis remained normal. The reoccurrence of the MDS-like phenotype in the secondary wild-type recipients supports the notion of the niche-

Figure 6. (continued) 1.0 mm. (D) Representative H&E-stained femoral sections showed increased MKs in the BM of the *Sipa1*$^{-/-}$ recipient mice. Scale bars represent 50 μm (black) and 25 μm (white). (E) The increased numbers of MKs in the *Sipa1*$^{-/-}$ recipient bone sections. The data are expressed as numbers per squared millimeters. (F) The frequencies of HSPCs in the recipient BM at the endpoint of the experiments. (G) H&E-stained spleen sections of *Sipa1*$^{+/+}$ and *Sipa1*$^{-/-}$ recipients 9 months after transplantation. Scale bars represent 1.0 mm for the upper panels and 50 μm for the lower panels. (H) Representative FACS profile showing gating strategy for HSPCs in spleen of *Sipa1*$^{+/+}$ and *Sipa1*$^{-/-}$ recipients 7 to 9 months after transplantation. (I) Frequencies of HSPCs in spleens of the *Sipa1*$^{+/+}$ and *Sipa1*$^{-/-}$ recipients. (J) Reduced mature blood cells in the PB of secondary recipients 6 months after transplantation of the spleen cells from a primary *Sipa1*$^{-/-}$ recipient with MPN. (K) The spleen weight of the secondary recipient mice 6 months after transplantation. The statistical differences in panels B-K were determined by nonparametric Mann-Whitney *U* test or parametric Student *t* test with Welch's correction according the data distribution. See also in supplemental Figure 4. KIT, CD117 or Proto-Oncogene C-Kit; WT, wild type.

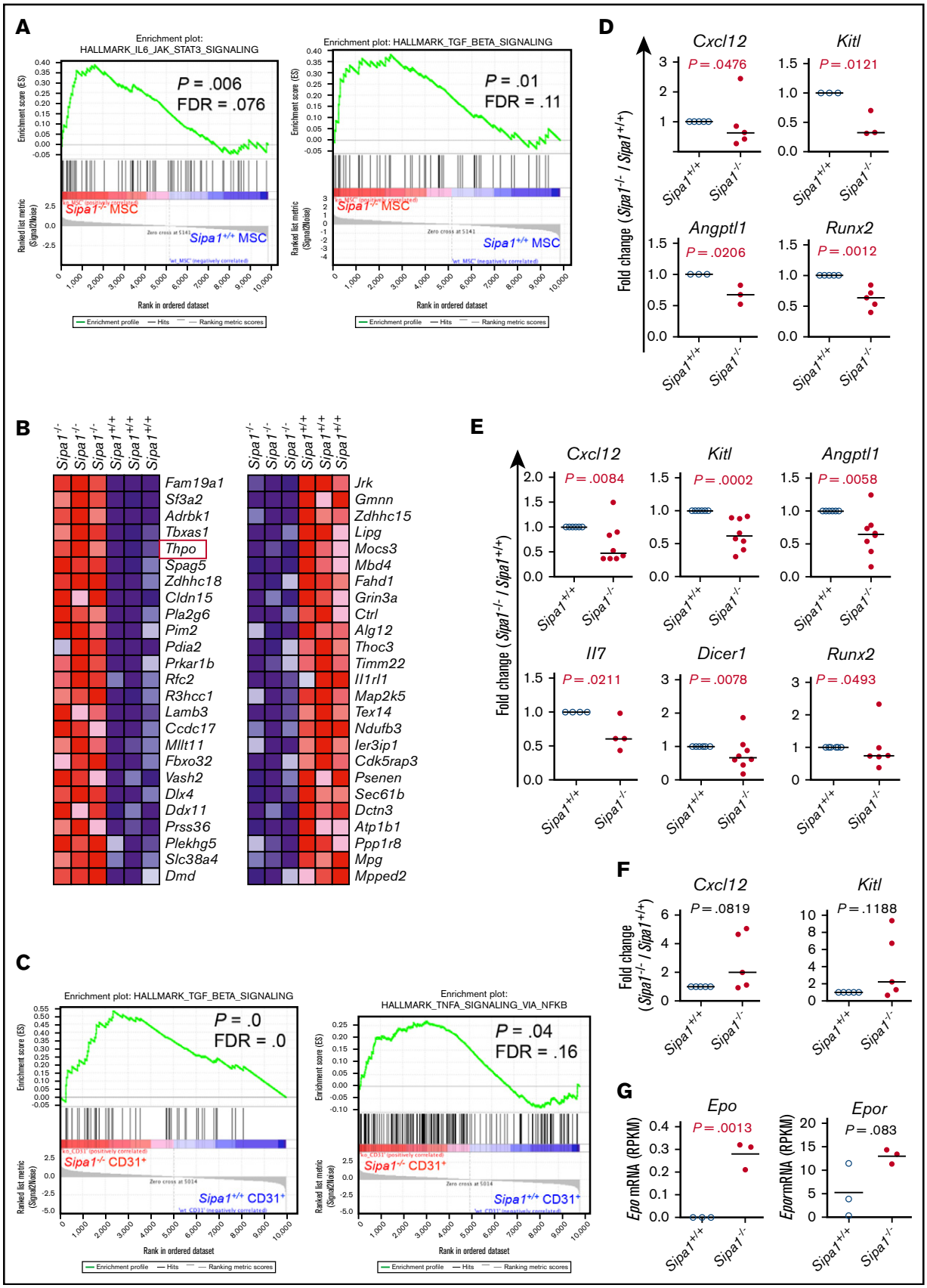

Figure 7.

induced malignant transformation of the donor cells. The disease phenotype is likely due to potential epigenetic alterations or selection of clonal hematopoiesis in the donor hematopoietic cells. However, the exact underlying mechanisms require further investigation in the future.

Understanding the molecular mechanisms mediating the niche-induced MPN is fundamental for identifying predicting factors for leukemogenesis. The increased expression of proinflammatory cytokines like TGF-β and TNF-α is a common feature of mouse models with MPN.[2] This was also observed in patients with MPN.[46,47] IL6/JAK/STAT3 signaling has been implicated in MPN progression.[48-52] The elevated IL-6, TGF-β, and TNF-α signaling pathways in the *Sipa1*$^{-/-}$ stromal cells may contribute to myeloproliferation possibly via altering HSC lineage fate decision in the *Sipa1*$^{-/-}$ mice, as previously suggested.[50,53]

THPO-MPL signaling is critical for maintaining HSCs in adult BM[54] and is involved in the pathogenesis of MPN.[55,56] The upregulation of *Thpo* in the *Sipa1*$^{-/-}$ BM stromal cells may be associated with the enhanced granulopoiesis and the overproduction of MEPs and MK hyperplasia in the aged *Sipa1*$^{-/-}$ mice under steady state and after transplantation. The increased number of MKs in BM might in turn promote the progression of the MDS/MPN via platelet factor secretion, as described recently.[57] In addition, it has been shown that EPO can direct multipotent HSPCs toward committed erythrocyte progenitors.[58] The increased *Epo* gene expression in *Sipa1*$^{-/-}$ endothelial cells might also contribute to the increase of MEPs.[57]

Il7 is critical for maintaining normal lymphopoiesis in adult mice.[59] The reduced *Il7* expression in the *Sipa1*$^{-/-}$ MPCs could indirectly lead to myeloproliferation in the *Sipa1*$^{-/-}$ recipients after transplantation. Furthermore, *Cxcl12*, *Kitl*, and *Angptl1* are critical to maintain normal hematopoiesis through keeping HSC quiescence,[5,40,60,61] and the reduction of these genes in BM niche cells were detected in previous MPN mouse models.[29,62] The downregulation of these genes in the *Sipa1*$^{-/-}$ MSCs and MPCs could affect HSC retention and quiescence and eventually promote the myelopoiesis. Deletion of *Dicer1* from osteoprogenitors leads to the development of MDS and AML.[9] Thus, the downregulation of *Dicer1* in the *Sipa1*$^{-/-}$ MPCs, enriched with osteoblast progenitors,[31] might contribute to the niche alteration and initiation of the MPN in the *Sipa1*$^{-/-}$ mice.

In conclusion, we have demonstrated that *Sipa1* loss in the BM stromal cells results in BM niche alterations, which are absolutely required for the development of MDS/MPN. The enhanced inflammatory cytokine signaling and myelopoiesis-promoting activities in the *Sipa1*$^{-/-}$ BM niche may have contributed to the disease pathogenesis. Our data provide novel evidence for niche-driven MPN and the underlying cellular and molecular mechanisms.

Acknowledgments

The authors are grateful to Minna Taipale and Andranik Durgaryan at Karolinska Institute and Liseotte Lenner at Linköping University for their technical assistance. All major computations were performed on resources provided by the Swedish National Infrastructure for Computing through Uppsala Multidisciplinary Center for Advanced Computational Science under Project b2014299. The authors acknowledge the MedH Core Flow Cytometry facility (Karolinska Institute) for providing cell-sorting/analysis services.

This study was supported by Swedish Research Council (K2013-99X-22241-01-5), Swedish Childhood Society (TJ2013-0048, PR2015-0142, and PROJ12/081), Swedish Cancer Society (CAN 2009/1589 and CAN 2012/891), Åke Olsson Foundation, Radiumhemmets Forskningsfonder, and Karolinska Institute Wallenberg Institute for Regenerative Medicine (H.Q.), and Knut and Alice Wallenbergs Foundation (M.S.).

Authorship

Contribution: H.Q. and P.X. designed, performed, analyzed data and wrote the manuscript; M. Dolinska, L.S., M.K., A.-S.J., M. Dimitriou, and T.B. assisted part of the study and manuscript review; Y.Z. performed μCT analysis and wrote the corresponding method in the manuscript; X.L. analyzed RNA sequencing data and wrote the corresponding method in the manuscript; N.M. provided the *Sipa1*$^{-/-}$ mice; G.Z.R. provided the morphologic assessment of histologic and cytologic preparations; D.T.S., E.H.-L., and J.W. provided scientific input on the study and manuscript review; M.S. performed the RNA and exome sequencing experiments and provided scientific input, and all authors have read and approved the manuscript.

Conflict-of-interest disclosure: The authors declare no competing financial interests.

ORCID profiles: P.X., 0000-0003-1308-4357; E.H.-L., 0000-0002-7839-3743; J.W., 0000-0002-5038-5063; M.S., 0000-0001-8527-7276; H.Q., 0000-0002-2512-9199.

Correspondence: Hong Qian, Center for Hematology and Regenerative Medicine, Department of Medicine, Karolinska Institute, Karolinska University Hospital, SE-141 86 Stockholm, Sweden; e-mail: hong.qian@ki.se.

Figure 7. Altered molecular profiles of BM stromal cell subsets in *Sipa1*$^{-/-}$ young adult mice. Gene set enrichment analysis was carried out on the RNA-sequencing data to identify differentially expressed genes in the *Sipa1*$^{-/-}$ stromal cells. The RNA sequencing was performed on FACS-sorted BM MSCs, MPCs, and endothelial cells from 2 to 3-month-old mice. Data were from 3 independent experiments. False discovery rate-q value represents the false discovery rate of the *P* value. (A) Upregulated IL-6/JAK2/STAT3 and TGF-β signaling pathways in the *Sipa1*$^{-/-}$ MSCs vs *Sipa1*$^{+/+}$ MSCs. (B) The top 25 altered genes in the *Sipa1*$^{-/-}$ MPCs relative to that in the *Sipa1*$^{+/+}$ mice. The red frame highlights *Thpo* gene. Red indicates high expression, and blue indicates low expression. (C) Enhanced TGF-β and TNF-α signaling in the *Sipa1*$^{-/-}$ endothelial cells. (D) qPCR analysis of *Kitl*, *Angptl1*, *Cxcl12*, and *Runx2* expressions in *Sipa1*$^{+/+}$ and *Sipa1*$^{-/-}$ MSCs. (E) qPCR analysis of *Kitl*, *Angptl1*, *Il7*, *Cxcl12*, *Dicer1*, and *Runx2* expressions in *Sipa1*$^{+/+}$ and *Sipa1*$^{-/-}$ MPCs. (F) qPCR analysis of *Kitl* and *Cxcl12* expressions in *Sipa1*$^{+/+}$ and *Sipa1*$^{-/-}$ endothelial cells. The statistical differences in panels D-F were analyzed by unpaired Mann-Whitney *U* test or Kolmogorov-Smirnov test. (G) RNA sequencing revealed upregulation of *Epo* and *Epor* in the *Sipa1*$^{-/-}$ endothelial cells. *P* values were calculated by unpaired Student *t* test. See also in supplemental Figures 5 and 6.

References

1. Schofield R. The relationship between the spleen colony-forming cell and the haemopoietic stem cell. *Blood Cells*. 1978;4(1-2):7-25.
2. Hoggatt J, Kfoury Y, Scadden DT. Hematopoietic stem cell niche in health and disease. *Annu Rev Pathol*. 2016;11:555-581.
3. Boulais PE, Frenette PS. Making sense of hematopoietic stem cell niches. *Blood*. 2015;125(17):2621-2629.
4. Pittenger MF, Mackay AM, Beck SC, et al. Multilineage potential of adult human mesenchymal stem cells. *Science*. 1999;284(5411):143-147.
5. Omatsu Y, Sugiyama T, Kohara H, et al. The essential functions of adipo-osteogenic progenitors as the hematopoietic stem and progenitor cell niche. *Immunity*. 2010;33(3):387-399.
6. Walkley CR, Shea JM, Sims NA, Purton LE, Orkin SH. Rb regulates interactions between hematopoietic stem cells and their bone marrow microenvironment. *Cell*. 2007;129(6):1081-1095.
7. Walkley CR, McArthur GA, Purton LE. Cell division and hematopoietic stem cells: not always exhausting. *Cell Cycle*. 2005;4(7):893-896.
8. Walkley CR, Olsen GH, Dworkin S, et al. A microenvironment-induced myeloproliferative syndrome caused by retinoic acid receptor gamma deficiency. *Cell*. 2007;129(6):1097-1110.
9. Raaijmakers MH, Mukherjee S, Guo S, et al. Bone progenitor dysfunction induces myelodysplasia and secondary leukaemia. *Nature*. 2010;464(7290):852-857.
10. Wang L, Zhang H, Rodriguez S, et al. Notch-dependent repression of miR-155 in the bone marrow niche regulates hematopoiesis in an NF-κB-dependent manner. *Cell Stem Cell*. 2014;15(1):51-65.
11. Dong L, Yu WM, Zheng H, et al. Leukaemogenic effects of Ptpn11 activating mutations in the stem cell microenvironment. *Nature*. 2016;539(7628):304-308.
12. Minato N, Hattori M. Spa-1 (Sipa1) and Rap signaling in leukemia and cancer metastasis. *Cancer Sci*. 2009;100(1):17-23.
13. Jin A, Kurosu T, Tsuji K, et al. BCR/ABL and IL-3 activate Rap1 to stimulate the B-Raf/MEK/Erk and Akt signaling pathways and to regulate proliferation, apoptosis, and adhesion. *Oncogene*. 2006;25(31):4332-4340.
14. Kometani K, Ishida D, Hattori M, Minato N. Rap1 and SPA-1 in hematologic malignancy. *Trends Mol Med*. 2004;10(8):401-408.
15. Ishida D, Kometani K, Yang H, et al. Myeloproliferative stem cell disorders by deregulated Rap1 activation in SPA-1-deficient mice. *Cancer Cell*. 2003;4(1):55-65.
16. Kurachi H, Wada Y, Tsukamoto N, et al. Human SPA-1 gene product selectively expressed in lymphoid tissues is a specific GTPase-activating protein for Rap1 and Rap2. Segregate expression profiles from a rap1GAP gene product. *J Biol Chem*. 1997;272(44):28081-28088.
17. Largaespada DA. A bad rap: Rap1 signaling and oncogenesis. *Cancer Cell*. 2003;4(1):3-4.
18. Altschuler DL, Ribeiro-Neto F. Mitogenic and oncogenic properties of the small G protein Rap1b. *Proc Natl Acad Sci USA*. 1998;95(13):7475-7479.
19. Brooks R, Kizer N, Nguyen L, et al. Polymorphisms in MMP9 and SIPA1 are associated with increased risk of nodal metastases in early-stage cervical cancer. *Gynecol Oncol*. 2010;116(3):539-543.
20. Yi SM, Li GY. The association of SIPA1 gene polymorphisms with breast cancer risk: evidence from published studies. *Tumour Biol*. 2014;35(1):441-445.
21. Ugenskienė R, Myrzaliyeva D, Jankauskaitė R, et al. The contribution of SIPA1 and RRP1B germline polymorphisms to breast cancer phenotype, lymph node status and survival in a group of Lithuanian young breast cancer patients. *Biomarkers*. 2016;21(4):363-370.
22. Yoshida N, Yagasaki H, Takahashi Y, Kudo K, Manabe A, Kojima S. Mutation analysis of SIPA1 in patients with juvenile myelomonocytic leukemia. *Br J Haematol*. 2008;142(5):850-851.
23. Arber DA, Orazi A, Hasserjian R, et al. The 2016 revision to the World Health Organization classification of myeloid neoplasms and acute leukemia. *Blood*. 2016;127(20):2391-2405.
24. Dolnik A, Engelmann JC, Scharfenberger-Schmeer M, et al. Commonly altered genomic regions in acute myeloid leukemia are enriched for somatic mutations involved in chromatin remodeling and splicing. *Blood*. 2012;120(18):e83-e92.
25. Kometani K, Aoki M, Kawamata S, et al. Role of SPA-1 in phenotypes of chronic myelogenous leukemia induced by BCR-ABL-expressing hematopoietic progenitors in a mouse model. *Cancer Res*. 2006;66(20):9967-9976.
26. Vardiman JW, Thiele J, Arber DA, et al. The 2008 revision of the World Health Organization (WHO) classification of myeloid neoplasms and acute leukemia: rationale and important changes. *Blood*. 2009;114(5):937-951.
27. Qian H, Badaloni A, Chiara F, et al. Molecular characterization of prospectively isolated multipotent mesenchymal progenitors provides new insight into the cellular identity of mesenchymal stem cells in mouse bone marrow. *Mol Cell Biol*. 2013;33(4):661-677.
28. Qian H, Le Blanc K, Sigvardsson M. Primary mesenchymal stem and progenitor cells from bone marrow lack expression of CD44 protein. *J Biol Chem*. 2012;287(31):25795-25807.
29. Schepers K, Pietras EM, Reynaud D, et al. Myeloproliferative neoplasia remodels the endosteal bone marrow niche into a self-reinforcing leukemic niche. *Cell Stem Cell*. 2013;13(3):285-299.
30. Méndez-Ferrer S, Michurina TV, Ferraro F, et al. Mesenchymal and haematopoietic stem cells form a unique bone marrow niche. *Nature*. 2010;466(7308):829-834.
31. Schepers K, Hsiao EC, Garg T, Scott MJ, Passegué E. Activated Gs signaling in osteoblastic cells alters the hematopoietic stem cell niche in mice. *Blood*. 2012;120(17):3425-3435.
32. Kogan SC, Ward JM, Anver MR, et al; Hematopathology Subcommittee of the Mouse Models of Human Cancers Consortium. Bethesda proposals for classification of nonlymphoid hematopoietic neoplasms in mice. *Blood*. 2002;100(1):238-245.

33. Bumm TG, Elsea C, Corbin AS, et al. Characterization of murine JAK2V617F-positive myeloproliferative disease. *Cancer Res*. 2006;66(23): 11156-11165.

34. Hasan S, Lacout C, Marty C, et al. JAK2V617F expression in mice amplifies early hematopoietic cells and gives them a competitive advantage that is hampered by IFNα. *Blood*. 2013;122(8):1464-1477.

35. Padron E. Surveying the landscape of MDS/MPN research: overlap among the overlap syndromes? *Hematology Am Soc Hematol Educ Program*. 2015; 2015:349-354.

36. Vardiman J, Hyjek E. World Health Organization classification, evaluation, and genetics of the myeloproliferative neoplasm variants. *Hematology Am Soc Hematol Educ Program*. 2011;2011:250-256.

37. Fialkow PJ, Jacobson RJ, Papayannopoulou T. Chronic myelocytic leukemia: clonal origin in a stem cell common to the granulocyte, erythrocyte, platelet and monocyte/macrophage. *Am J Med*. 1977;63(1):125-130.

38. Ding L, Morrison SJ. Haematopoietic stem cells and early lymphoid progenitors occupy distinct bone marrow niches [published correction appears in Nature. 2014;514(7521):262]. *Nature*. 2013;495(7440):231-235.

39. Ding L, Saunders TL, Enikolopov G, Morrison SJ. Endothelial and perivascular cells maintain haematopoietic stem cells. *Nature*. 2012;481(7382):457-462.

40. Greenbaum A, Hsu YM, Day RB, et al. CXCL12 in early mesenchymal progenitors is required for haematopoietic stem-cell maintenance. *Nature*. 2013; 495(7440):227-230.

41. Sugiyama T, Kohara H, Noda M, Nagasawa T. Maintenance of the hematopoietic stem cell pool by CXCL12-CXCR4 chemokine signaling in bone marrow stromal cell niches. *Immunity*. 2006;25(6):977-988.

42. Akhter S, Rahman MM, Lee HS, Kim HJ, Hong ST. Dynamic roles of angiopoietin-like proteins 1, 2, 3, 4, 6 and 7 in the survival and enhancement of ex vivo expansion of bone-marrow hematopoietic stem cells. *Protein Cell*. 2013;4(3):220-230.

43. Jilka RL, Takahashi K, Munshi M, Williams DC, Roberson PK, Manolagas SC. Loss of estrogen upregulates osteoblastogenesis in the murine bone marrow. Evidence for autonomy from factors released during bone resorption. *J Clin Invest*. 1998;101(9):1942-1950.

44. Zanotti S, Kalajzic I, Aguila HL, Canalis E. Sex and genetic factors determine osteoblastic differentiation potential of murine bone marrow stromal cells. *PLoS One*. 2014;9(1):e86757.

45. Lane SW, Wang YJ, Lo Celso C, et al. Differential niche and Wnt requirements during acute myeloid leukemia progression. *Blood*. 2011;118(10): 2849-2856.

46. Tefferi A, Vaidya R, Caramazza D, Finke C, Lasho T, Pardanani A. Circulating interleukin (IL)-8, IL-2R, IL-12, and IL-15 levels are independently prognostic in primary myelofibrosis: a comprehensive cytokine profiling study. *J Clin Oncol*. 2011;29(10):1356-1363.

47. Ciurea SO, Merchant D, Mahmud N, et al. Pivotal contributions of megakaryocytes to the biology of idiopathic myelofibrosis. *Blood*. 2007;110(3):986-993.

48. Cokic VP, Mitrovic-Ajtic O, Beleslin-Cokic BB, et al. Proinflammatory cytokine IL-6 and JAK-STAT signaling pathway in myeloproliferative neoplasms. *Mediators Inflamm*. 2015;2015:453020.

49. Sansone P, Bromberg J. Targeting the interleukin-6/Jak/stat pathway in human malignancies. *J Clin Oncol*. 2012;30(9):1005-1014.

50. Reynaud D, Pietras E, Barry-Holson K, et al. IL-6 controls leukemic multipotent progenitor cell fate and contributes to chronic myelogenous leukemia development. *Cancer Cell*. 2011;20(5):661-673.

51. Kleppe M, Kwak M, Koppikar P, et al. JAK-STAT pathway activation in malignant and nonmalignant cells contributes to MPN pathogenesis and therapeutic response. *Cancer Discov*. 2015;5(3):316-331.

52. Welner RS, Amabile G, Bararia D, et al. Treatment of chronic myelogenous leukemia by blocking cytokine alterations found in normal stem and progenitor cells. *Cancer Cell*. 2015;27(5):671-681.

53. Mirantes C, Passegué E, Pietras EM. Pro-inflammatory cytokines: emerging players regulating HSC function in normal and diseased hematopoiesis. *Exp Cell Res*. 2014;329(2):248-254.

54. Qian H, Buza-Vidas N, Hyland CD, et al. Critical role of thrombopoietin in maintaining adult quiescent hematopoietic stem cells. *Cell Stem Cell*. 2007; 1(6):671-684.

55. Drexler HG, Quentmeier H. Thrombopoietin: expression of its receptor MPL and proliferative effects on leukemic cells. *Leukemia*. 1996;10(9): 1405-1421.

56. Hirai H, Shimazaki C, Yamagata N, et al. Effects of thrombopoietin (c-mpl ligand) on growth of blast cells from patients with transient abnormal myelopoiesis and acute myeloblastic leukemia. *Eur J Haematol*. 1997;59(1):38-46.

57. Zhan H, Ma Y, Lin CH, Kaushansky K. $JAK2^{V617F}$-mutant megakaryocytes contribute to hematopoietic stem/progenitor cell expansion in a model of murine myeloproliferation. *Leukemia*. 2016;30(12):2332-2341.

58. Grover A, Mancini E, Moore S, et al. Erythropoietin guides multipotent hematopoietic progenitor cells toward an erythroid fate. *J Exp Med*. 2014;211(2):181-188.

59. Tsapogas P, Zandi S, Åhsberg J, et al. IL-7 mediates Ebf-1-dependent lineage restriction in early lymphoid progenitors. *Blood*. 2011;118(5):1283-1290.

60. Arai F, Hirao A, Ohmura M, et al. Tie2/angiopoietin-1 signaling regulates hematopoietic stem cell quiescence in the bone marrow niche. *Cell*. 2004; 118(2):149-161.

61. Thorén LA, Liuba K, Bryder D, et al. Kit regulates maintenance of quiescent hematopoietic stem cells. *J Immunol*. 2008;180(4):2045-2053.

62. Arranz L, Sánchez-Aguilera A, Martín-Pérez D, et al. Neuropathy of haematopoietic stem cell niche is essential for myeloproliferative neoplasms. *Nature*. 2014;512(7512):78-81.